Compensation for Joule-Thomson effect in flowrate measurements by GMDH polynomial

Ivan Maric, Ivan Ivek

Rudjer Boskovic Institute, Laboratory for information systems, Bijenicka 54, 10002 Zagreb, Croatia

Abstract

The international standard for flowrate measurements ISO-5167 recommends the temperature sensor to be located downstream of the differential device what may cause a significant error in the measurement of the flowrate of natural gas, especially at high differential pressure, low temperature and low diameter ratio. The flowrate generally needs to be compensated for the temperature change due to the Joule-Thomson effect caused by the constriction of the metering device. The accurate compensation involves double calculation of both the natural gas properties and the flowrate. To decrease the computational load, an automatic correction of the flowrate by the GMDH polynomial surrogate is proposed. By using the compound measure of the approximation error and the execution time for model selection, the modified GMDH algorithm searches for the satisfactory model fulfilling the constraints of real-time application. The automatic correction of the flowrate measurements of a natural gas is simulated and the corresponding results are discussed. The derived model can be equally used for a natural gas specified by composition or by physical properties.

Keywords: Flowrate measurements, Real-time systems, Modeling, Embedded systems

1. Introduction

The international standard ISO-5167 [1] specifies the calculation of the flowrate by using the upstream temperature and upstream pressure of the fluid but it also suggests the temperature should be preferably measured downstream of the primary device. When positioning the temperature sensor downstream of the differential device, the measured flowrate of gaseous fluid generally needs to be compensated for the temperature change due to the Joule-Thomson (JT) effect caused by the constriction of the primary device. The measurement error may increase significantly, especially at high differential pressure, low temperature and at low diameter ratio [2].

Fig. 1 shows the schematic diagram of the natural gas flowrate measurement using an orifice plate with corner taps [3]. The temperature of the natural gas flowing through an orifice changes due to the JT effect. The procedure for the compensation of JT effect includes the calculation of thermodynamic properties of the natural gas [4]-[6], requiring a substantial computing power in order to be executable in real-time.

The temperature change ΔT is defined by the following relation [1]:

$$\Delta T = T_u - T_d = \mu_{JT} \cdot \Delta\omega, \qquad (1)$$

where T_u and T_d denote the corresponding upstream and downstream temperature, μ_{JT} denotes the JT coefficient and $\Delta\omega$ is the pressure loss. The computation of the JT coefficient of the natural gas [2][5][6] is a time consuming procedure and generally includes the calculation of the corresponding density [7][8][9]. The approximate equation for pressure loss [10]

$$\Delta\omega = \frac{\sqrt{1-\beta^4\left(1-C^2\right)}-C\beta^2}{\sqrt{1-\beta^4\left(1-C^2\right)}+C\beta^2}\Delta p \qquad (2)$$

relates the pressure loss $\Delta\omega$ to differential pressure Δp, the discharge coefficient C and the ratio $\beta=d/D$ between the internal diameters of the primary device (d) and the pipe (D). From Eqs. (1) and (2) it is obvious that the temperature drop ΔT is directly proportional to the differential pressure Δp.
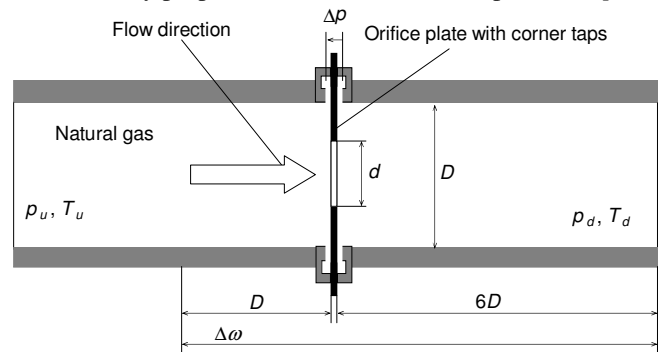

Fig. 1. The schematic diagram of the natural gas flowrate measurement [3] using an orifice plate with corner taps

The following section describes a computationally intensive procedure for the precise compensation of the flowrate error caused by the temperature change. We aim to build a low complexity GMDH model for the flowrate correction procedure and in this manner make the correction feasible in real-time in low-computing power systems. In Section 3 a brief description of the GMDH algorithm is given. Then the preparation of training and validation data (Section 4), followed by the elimination of insignificant parameters (Section 5) is given. Finally, the construction of the

corresponding GMDH surrogate is described in Section 6 and the results of the simulations of the flowrate measurements are presented in Section 7.

Nomenclature		
Symbol	Meaning	Units
C	coefficient of discharge	
d	diameter of orifice of primary device	m
D	upstream internal pipe diameter	m
H_S	superior calorific value [gas at normal conditions (0 ºC, 101325 bar), combustion temperature 25 ºC]	MJ/m^3
K	flowrate correction factor	
p	absolute static pressure of the fluid	MPa
q	mass flowrate	kg/s
T	temperature	K
X	mole fraction	
β	diameter ratio $\beta=d/D$	
γ	dynamic viscosity of a gas under working conditions	Pa·s
Δp	differential pressure	MPa
$\Delta\omega$	pressure loss	MPa
κ	isentropic exponent	
μ	Joule-Thomson coefficient	K/MPa
ρ	density of the fluid	kg/m^3
ρ_r	relative density [gas at normal conditions (0 ºC, 101325 bar)]	
Subscripts		
u	upstream conditions	
d	downstream conditions	
$GMDH$	Approximation by GMDH	

2. Flowrate correction procedure

According to [1] and [3], the calculation of the natural gas flowrate depends on multiple parameters:

$$q_u = q\left(P_u, T_u, \Delta p, \rho_u, \gamma_u, \kappa_u, D, d\right) , \qquad (3)$$

where q_u, ρ_u, γ_u and κ_u represent the corresponding mass flowrate, density, viscosity and the isentropic exponent calculated at upstream pressure P_u and temperature T_u, while D and d denote the internal diameters of the pipe and the orifice, respectively. In case of the upstream pressure and the downstream temperature measurement, as suggested by [1], the flowrate equation, Eq. (3), changes to:

$$q_d = q\left(P_u, T_d, \Delta p, \rho_d, \gamma_d, \kappa_d, D, d\right), \qquad (4)$$

where q_d, ρ_d, γ_d and κ_d denote the corresponding mass flowrate, density, viscosity and the isentropic exponent calculated in "*downstream conditions*" i.e. at the upstream pressure p_u and the downstream temperature T_d. For certain natural gas compositions and operating conditions the flowrate q_d may differ significantly from q_u and the corresponding compensation for the temperature change may be necessary in order to preserve the requested measurement accuracy.

The precise correction of the natural gas flowrate, based on the upstream pressure and the downstream temperature measurement, Eq. (4), and on the computation of the corresponding natural gas properties, is summarized in Table

1. The procedure in Table 1 requires a double calculation of both the flowrate and the properties of the natural gas. To reduce the computational burden we aim to derive a low-complexity flowrate correction factor model that will enable direct compensation of the flowrate error caused by the measurement of the downstream temperature. The correction factor model has to be simple enough in order to be executable in real-time and accurate enough to ensure acceptable measurement accuracy.

Table 1

Precise correction of the flowrate of the natural gas based on the downstream temperature measurement and on the computation of the natural gas properties

Step	Description
1	Calculate the natural gas properties (ρ_d [7], μ_{JT} [6] and κ_d [6]) at p_u, and T_d
2	Calculate the dynamic viscosity γ_d at P_u, and T_d (e.g. by using the residual viscosity equation [11])
3	Calculate the mass flowrate q_d and the discharge coefficient C [3] at P_u, and T_d (Eq. (4))
4	Calculate the pressure loss $\Delta\omega$ (Eq. (2))
5	Calculate the upstream temperature T_u in accordance with Eq. (1)
6	Calculate the the natural gas properties (ρ_u [7] and κ_u [6]) at p_u, and T_u
7	Calculate the viscosity γ_u at p_u, and T_u (e.g. by using the residual viscosity equation [11])
8	Calculate the mass flowrate q_u [3] at p_u, and T_u (Eq. (3))

The flowrate correction factor K can be obtained by dividing the true flowrate q_u calculated in the upstream conditions, Eq. (3), by the flowrate q_d calculated in the "*downstream conditions*", Eq. (4):

$$K = \frac{q_u}{q_d} . \qquad (5)$$

For the given correction factor (5), the flowrate at the upstream pressure and temperature can be calculated directly from the flowrate computed in the "*downstream conditions*", i.e. $q_u = K \cdot q_d$. Our objective is to derive the GMDH polynomial model of the flowrate correction factor. Given the GMDH surrogate (K_{GMDH}) for the flowrate correction factor Eq. (5), the true flowrate q_u can be approximated by: $q_{GMDH} = K_{GMDH} \cdot q_d$, where q_{GMDH} denotes the corrected flowrate. The following section contains a brief description of the GMDH algorithm and the compound error measure for the model selection.

3. GMDH algorithm

Approximation of complex multidimensional systems by self-organizing polynomials, also known as the Group Method of Data Handling (GMDH), was introduced by A.G. Ivakhnenko [12]-[14]. The GMDH models are constructed by combining the low-order polynomials into multi layered polynomial networks. GMDH polynomials may achieve high approximation accuracy at low complexity and are simple to implement in digital computers. Fig. 2 illustrates a complete

2-layer feed-forward GMDH network representing a 3-dimensional system, where $p_{\lambda,i}$ denotes a two-dimensional polynomial corresponding to the ith node of the layer λ.
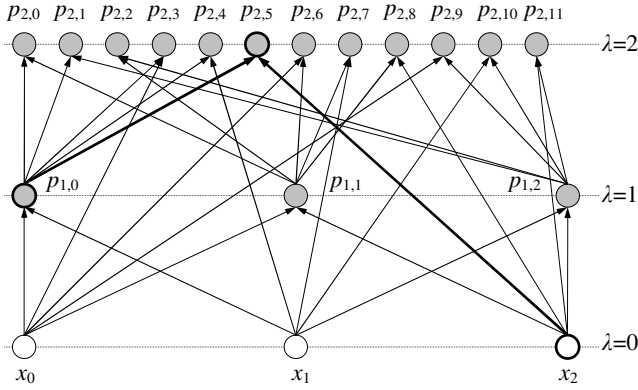

Fig. 2. Illustration of GMDH polynomials construction

In our implementation of the GMDH algorithm a two-dimensional second-order polynomial

$$p_{\lambda i} = a_{\lambda i0} + a_{\lambda i1} z_{\lambda i1} + a_{\lambda i2} z_{\lambda i2} + a_{\lambda i3} z_{\lambda i1}^2 + a_{\lambda i4} z_{\lambda i2}^2 + a_{\lambda i5} z_{\lambda i1} z_{\lambda i2} \quad (6)$$

is implemented, where $z_{\lambda i1}$ and $z_{\lambda i2}$ represent the input variables and $a_{\lambda i0},...,a_{\lambda i5}$ are the corresponding coefficients obtained by the polynomial regression. Note that $z_{\lambda i1}$ and $z_{\lambda i2}$ can be any combination of two different variables from the lower layers including the initial zero-layer variables (x_i) and the derived regression polynomials ($p_{\lambda,i}$). For example, the input variables for the polynomial $p_{2,5}$ from Fig. 2 are the polynomial $p_{1,0}$ from the 1st layer and the initial variable x_2.

The GMDH algorithm assumes two independent data sets: a training set of M samples

$$\mathcal{D}_t = \{(\mathbf{x}_{ti}, y_{ti})\}_{i=1}^{M}, \quad (7)$$

where each sample consists of a data vector $\mathbf{x}_{ti} = (x_{ti_1}, x_{ti_2},...,x_{ti_K})$, $x_{ti} \in \mathcal{R}^K$, and the corresponding dependent variable $y_{ti} \in \mathcal{R}$, as well a validation data set of N samples

$$\mathcal{D}_v = \{(\mathbf{x}_{vi}, y_{vi})\}_{i=1}^{N}, \quad (8)$$

where each sample consists of a data vector $\mathbf{x}_{vi} = (x_{vi_1}, x_{vi_2},...,x_{vi_K})$, $x_{vi} \in \mathcal{R}^K$, with the corresponding dependent variable $y_{vi} \in \mathcal{R}$. The algorithm uses the training data set, Eq. (7), to fit the coefficients of the regression polynomial and the validation set, Eq. (8), to verify the approximation error of the polynomial. The polynomials are then ranked according to the predefined performance measure.

In order to calculate the regression coefficients, $a_{\lambda i0},...,a_{\lambda i5}$, by polynomial regression, a set of 6 simultaneous linear equations

$$\left\{ \frac{\partial}{\partial a_{\lambda ik}} \sum_{m=1}^{M} (y_{tm} - p_{\lambda i}(t,m))^2 = 0 \right\}_{k=0}^{5}, \quad (9)$$

must be solved, where M is a total number of training samples, y_{tm} is the mth sample value of the dependent variable from the training data set, Eq. (7), and $p_{\lambda i}(t,m)$ is the value of the ith polynomial at layer λ corresponding to the mth data vector from the training data set. In our implementation of the GMDH algorithm the above set of linear equations is solved by the Gauss elimination method using forward elimination, back substitution, and pivoting [15].

In order for it to be applicable to real-time measurement systems the surrogate model of the complex calculation procedure must satisfy the requirements regarding the accuracy and the execution time, the most critical parameters in real-time measurements. We define the following requirements:

$$E_{rrs} \le E_{rrs0} \ \& \ T_{exe} \le T_{exe0} \quad (10)$$

where E_{rrs} and T_{exe} denote the corresponding Root Relative Squared Error (RRSE) and the estimated Execution Time (ET) of the model while E_{rrs0} and T_{exe0} represent their respective thresholds.

When modeling the complex multidimensional system by using the GMDH algorithm the total number of possible models may increase immensely by increasing the number of layers and the exhaustive search becomes unfeasible. It is generally necessary to restrict the search area by limiting the maximum number of possible candidate models per layer. The proper selection of candidate models plays an important role in building the satisfactory GMDH model. The Root Mean Squared Error (RMSE) measure is commonly used for the selection of the best candidate models as it selects the models with the minimum approximation error. The RRSE is equivalent to RMSE measure because they are directly proportional. In our GMDH algorithm we employed the RRSE measure since the relative error is more frequently used for the characterization of the flow-computer accuracy than the absolute error. The RRSE measure is defined by:

$$E_{rrs} = \sqrt{\sum_{i=1}^{N} (p_{vi} - y_{vi})^2 \Big/ \sum_{i=1}^{N} (y_{vi} - \bar{y}_v)^2} \quad (11)$$

where p_{vi} denotes the approximation of the dependent variable y_{vi}, and $\bar{y}_v = \frac{1}{N} \sum_{i=1}^{N} y_{vi}$ denotes the mean value of the dependent variable from the validation data set.

A recent research [16] shows that the two-parameter measure, combining the RRSE and the ET, may discover more favorable models for real-time applications than the single error measure, since it optimizes the model with respect to both the approximation accuracy and the ET i.e. the complexity. The two-parameter Compound Error (CE) measure [16] is defined by:

$$E_{CE} = c_w \cdot \left(E_{rrs}/E_{rrs0}\right)^2 + \left(1 - c_w\right) \cdot \left(T_{exe}/T_{exe0}\right)^2, \qquad (12)$$

where c_w, ($0 \le c_w \le 1$) denotes the weighting coefficient. The CE measure Eq. (12) is searching for the model with minimum compound error having the RRSE and ET both below the corresponding thresholds Eq. (10). The CE measure Eq. (12) normalizes each parameter to the corresponding threshold and evaluates its contribution to the compound error. By varying the coefficient c_w the contribution of each term changes. The GMDH algorithm with RRSE and CE measure is used to model the flowrate correction factor Eq, (5). The following section describes the preparation of training and validation samples for the correction factor modeling.

4. Preparation of training and validation data

The density of the natural gas in industrial applications can be calculated by using the natural gas composition [7][9] or its physical properties [8][17][18]. Within the ranges of application for the pipeline quality gases, the ISO-12213-2 [7] (Table 2) and ISO-12213-3 [8] (Table 3) produce identical results for the compression factor Z and the density ρ within the 5 most significant digits.

The ranges of application of input parameters for the flowrate measurement based on orifice plates [3] are shown in Table 4. In addition to Table 4, some extra limitations regarding the ranges of application of intermediate parameters like the Reynolds number and the diameter ratio must also be satisfied [3]. Our idea is to derive the GMDH polynomial

Table 2

ISO-12213-2 input parameters with the ranges of application for pipeline quality gas

Index	Parameter description		Range of application
0		nitrogen	$0 \le X_{N2} \le 0.20$
1		carbon dioxide	$0 \le X_{CO2} \le 0.20$
2		methane	$0 \le X_{CH4} \le 1.00$
3		ethane	$0 \le X_{C2H6} \le 0.10$
4		propane	$0 \le X_{C3H8} \le 0.035$
5		n-butane	n-butane+iso-butane
6		iso-butane	$0 \le X_{C4H10} \le 0.015$
7		n-pentane	n-pentane+iso-pentane
8	Mole fraction of:	iso-pentane	$0 \le X_{C5H12} \le 0.005$
9		n-hexane	$0 \le X_{C6H14} \le 0.001$
10		n-heptane	$0 \le X_{C7H16} \le 0.0005$
11		n-octane	n-octane+n-nonane+n-decane
12		n-nonane	$0 \le X_{C8H18} + X_{C9H20} + X_{C10H22} \le$
13		n-decane	0.0005
14		hydrogen	$0 \le X_{H2} \le 0.10$
15		carbon monoxide	$0 \le X_{CO} \le 0.03$
16		water	$0 \le X_{H2O} \le 0.00015$
17		helium	$0 \le X_{He} \le 0.005$
18		oxygen	$0 \le X_{O2} \le 0.0002$
19		hydrogen sulfide	$0 \le X_{H2S} \le 0.0002$
20		argon	$0 \le X_{Ar} \le 0.0002$
21	Absolute pressure in MPa		$0 < p \le 12$
22	Temperature in K		$263 \le T \le 368$

(Total sum of mole fractions must be equal to 1.00)

Table 3

ISO-12213-3 input parameters with the ranges of application for pipeline quality gas

Index	Parameter description	Range of application
0	X_{CO2} - mole fraction of carbon dioxide	$0 \le X_{CO2} \le 0.20$
1	X_{H2} - mole fraction of hydrogen	$0 \le X_{H2} \le 0.10$
2	p - absolute pressure in MPa	$0 < p \le 12$
3	T - temperature in K	$263 \le T \le 368$
4	ρ_r - relative density	$0.55 \le d \le 0.80$
5	H_S - superior calorific value in MJ/m^3	$30 \le H_S \le 45$

Table 4

Ranges of application of input parameters for fluid flowrate measurements based on orifice plates with corner taps [3]

Index	Parameter description	Range of application
0	ρ - density in kg/m^3	not specified
1	γ - viscosity in Pa·s	not specified
2	κ - isentropic exponent	not specified
3	p - absolute pressure in MPa	not specified
4	T - temperature in K	not specified
5	Δp - differential pressure in MPa	$0 \le \Delta p \le 0.25p$
6	D - pipe diameter in mm	$50 \le D \le 1000$
7	d - orifice diameter in mm	$12.5 \le d \le 750$
8	β - diameter ratio	$0.1 \le \beta \le 0.75$

model of the correction factor Eq. (5) that could be used for the correction of the flowrate regardless of the procedure used for the calculation of the natural gas properties, [7] or [8]. In order to make it applicable for the natural gas specified by either [7] or [8] we need to select the representative parameters common to both procedures. Given that ISO-12213-2 and ISO-12213-3 procedures are equivalent within the specified operating conditions and since the ISO-12213-2 input parameters (Table 2) can be easily converted into the ISO-12213-3 input parameters (Table 3), the ISO-12213-3 input parameters can be thought of as representative for both procedures. In addition to ISO-12213-3 parameters, the parameters (Table 4)

Table 5

Complete set of input parameters for the calculation of natural gas flowrate

Index	Parameter description	Range of application
0	X_{CO2} - mole fraction of carbon dioxide	$0 \le X_{CO2} \le 0.20$
1	X_{H2} - mole fraction of hydrogen	$0 \le X_{H2} \le 0.10$
2	p - absolute pressure in MPa	$0 < p \le 12$
3	T - temperature in K	$263 \le T \le 368$
4	ρ_r - relative density	$0.55 \le \rho_r \le 0.80$
5	H_S - superior calorific value in MJ/m^3	$30 \le H_S \le 45$
6	ρ - density in kg/m^3	unspecified
7	γ - viscosity in Pa·s	unspecified
8	κ - isentropic exponent	unspecified
9	Δp - differential pressure in MPa	$0 \le \Delta p \le 0.25p \le 0.2$
10	D - pipe diameter in mm	$50 \le D \le 1000$
11	d - orifice diameter in mm	$12.5 \le d \le 750$
12	β - orifice to pipe diameter ratio: d/D	$0.1 \le \beta \le 0.75$

representing the ISO-5167-2 flowrate calculation procedure [3], need to be included. Hence, the complete set of input

parameters for the calculation of the flowrate is constructed from the parameters given in Table 3 and Table 4 and is shown in Table 5.

Table 6

Procedure for generation of training and validation data samples used for flowrate correction factor modeling

Step	Description
1	Set data sample counter
2	Generate randomly the parameters from Table 2 by satisfying the corresponding ranges of application
3	Use the procedure specified in [19] to calculate relative density (ρ_r) and the superior calorific value (H_S) at normal conditions
4	If (relative density (ρ_r) or the superior calorific value (H_S) out of range (Table 5)) Then go to Step 2 Else proceed
5	Generate randomly Δp, D and d by satisfying the corresponding ranges of application (Table 5)
6	Use the procedure specified in Table 1 to calculate the density (ρ), the viscosity (γ), the isentropic exponent (κ), the uncorrected (q_d) and the true (q_u) mass flowrate
7	Using Eq. (5) calculate the flowrate correction factor K
8	Save data sample: ($X_{CO2}, X_{H2}, p, T, \rho_r, H_S, \rho, \gamma, \kappa, \Delta p, D, d, \beta; K$) and decrement data sample counter
9	If (data sample counter equals zero) Then Exit Else go to Step 2

Note that we limited the maximum possible value of the differential pressure Δp to 0.2 MPa (Table 5). In order to facilitate the modeling of the correction factor, Eq. (5), we have randomly generated the training, Eq. (7), and the validation, Eq. (8), data set. The corresponding high accuracy procedure, involving the double calculation of the flowrate and the physical properties, is summarized in Table 6.

In the following step we will try to reduce the total number of necessary parameters by minimizing the effect of parameter removal on the accuracy of the correction factor model. Finally we aim to build the polynomial model of the correction factor by satisfying some predefined complexity and accuracy thresholds Eq. (12).

5. Elimination of insignificant parameters

The procedure for the removal of the least significant input parameters begins with the complete set of parameters (Table 5) by searching for the parameter, whose elimination results in the minimum RRSE of the corresponding best polynomial model obtained at the predefined layer and removes the parameter if the corresponding RRSE remains below the given error threshold. The procedure ends if none of the remaining parameters can be removed without causing the corresponding best model RRSE to exceed the predefined error threshold. Fig. 3 illustrates in log_{10} scale the average RRSE of the best 10 polynomial models obtained after the elimination of the corresponding parameter from the initial set of 13 parameters (Table 5). Fig. 3 shows that the pipe diameter P_d has the lowest and the differential pressure Dp the highest impact on the RRSE of all 13 input parameters.
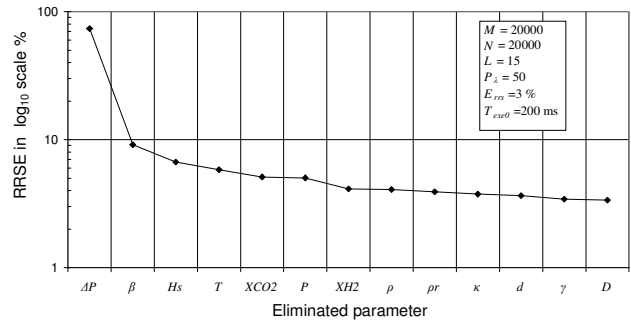

Fig. 3. Illustration of the effect of parameter removal on the RRSE of the corresponding best polynomial model. The corresponding RRSE is obtained after the elimination of each single parameter from the initial set of input parameters (Table 5). The best polynomials are all obtained at layer 15 by using GMDH algorithm with the RRSE selection criterion (11) and by retaining the best 50 models per each layer.

Fig. 4 shows the average compound error E_{CE}, Eq. (12), in log_{10} scale for the best 10 models obtained at layer 15 against the total number of the most significant parameters used for their generation. For example, the average E_{CE} for X_{CO2} corresponds to the models obtained by using all 5 leftmost parameters, i.e. Δp, β, H_S, T and X_{CO2}. The RRSE threshold equals 3%, the corresponding ET threshold is 200 ms, the average execution time of the basic GMDH polynomial, Eq. (6), equals 1 ms, the total number of models per layer is 50 and the maximum total number of layers is 15. The results are obtained by using the CE measure with the weighting coefficient c_w=0.5.
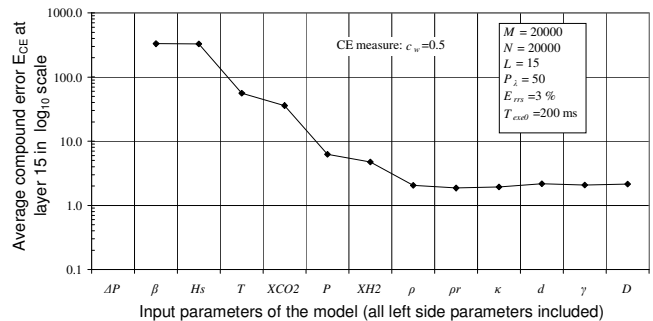

Fig. 4. Average CE (Eq. 12) for the 10 best models obtained at layer 15 against the total number of the most significant parameters used for their generation.

From Fig. 4 it can be seen that the best models (minimum E_{CE}) have been obtained by using the 9 most representative parameters from Table 5 (see Fig. 3), i.e. Δp, β, H_S, T, X_{CO2}, P, X_{H2}, ρ and ρ_r. It is also evident from Fig. 4 that the remaining least significant input parameters do not produce further decrease of compound error (E_{CE}) of the model. Almost identical outline has been obtained for the average RRSE of the best models. The optimal input parameters with the corresponding ranges of application are shown in Table 7.

Table 7
Optimal input parameters for the natural gas flowrate correction factor modeling

Index	Parameter description	Range of application
0	X_{CO2} - mole fraction of carbon dioxide	$0 \leq X_{CO2} \leq 0.20$
1	X_{H2} - mole fraction of hydrogen	$0 \leq X_{H2} \leq 0.10$
2	p - absolute pressure in MPa	$0 < p \leq 12$
3	T - temperature in K	$263 \leq T \leq 368$
4	Δp - differential pressure in MPa	$0 \leq \Delta p \leq 0.25p$
5	ρ - density in kg/m^3	unspecified
6	ρ_r - relative density	$9.55 \leq \rho_r \leq 0.80$
7	H_S - superior calorific value in MJ/m^3	$30 \leq H_S \leq 45$
8	β - orifice to pipe diameter ratio: d/D	$0.1 \leq \beta \leq 0.75$

The GMDH model of the flowrate correction factor, Eq. (5), relates the correction factor to the "*downstream conditions*" (p_u and T_d) and can be written in the following form:

$$K_{GMDH} = K_{GMDH}(x_{CO_2}, x_{H2}, p_u, T_d, \Delta p, \rho_d, \rho_r, H_S, \beta). \quad (13)$$

The limits of use of the GMDH correction factor are given in Table 7. The valid ranges of the Reynolds number are defined in [3] and for the orifice plates with corner taps are: $Re_D \geq 5000$ for $0.1 \leq \beta \leq 0.56$ and $Re_D \geq 16000 \cdot \beta^2$ for $\beta > 0.56$.

6. Flowrate correction factor modeling

The GMDH model of JT coefficient [16] enables an indirect compensation of a temperature drop and the corresponding flowrate error. The flowrate correction procedure [16] involves a double calculation of the flowrate of the natural gas. First, the flowrate is calculated using the "*downstream conditions*", than the JT coefficient is computed using its GMDH model, followed by the estimation of the temperature drop Eq. (1) and finally the corrected upstream temperature is used to calculate the flowrate precisely. In this paper we aim
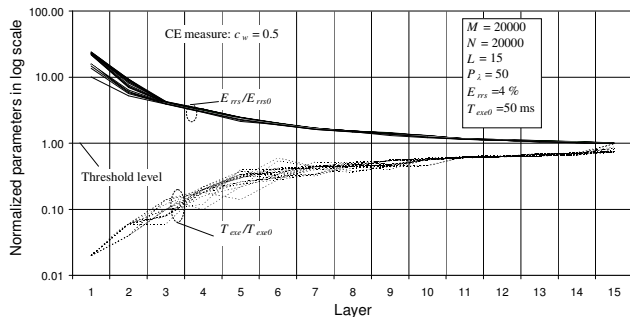
Fig. 5. Illustration of the GMDH algorithm approaching the error thresholds, Eq. (10), for the flowrate correction factor K by using the CE criterion, Eq. (12), with the weighting coefficient c_w=0.5. The RRSE (solid lines) and the ET (dotted lines) for the best 20 models at each layer are normalized to their respective thresholds. The algorithm uses the training and the validation data set each consisting of 20000 samples. The maximum number of qualified polynomials per layer is set to P_λ=50 for each layer λ=1,...,15, the average ET of the basic GMDH polynomial is set to 1 ms, and the thresholds, Eq. (10), are set to E_{rrs0}=4.0% and T_{exe0}=50ms. The RRSE for at least one model at layer 15 drops below the threshold before the corresponding ET exceeds it and the algorithm finds the satisfactory model.

to derive a GMDH surrogate of a complex correction procedure (Table 1) in order to reduce the complete procedure to a single multiplication between the flowrate, measured in the "*downstream conditions*", and the GMDH substitute of the correction factor Eq. (13). The precise compensation procedure (Table 1) will be translated into the GMDH surrogate by using two-parameter measure, Eq. (12), for model selection. Using GMDH algorithm [16] different models can be obtained by varying the total number of the most favorable candidate models that are retained per layer and the error thresholds for RRSE and ET of the model. The GMDH model of the flowrate correction factor will be tailored for the FC prototype based on low-power 8-bit/16-MHz MPU (Z84C15) with no hardware support for floating-point (FP) operations. The embedded FP package enables the calculation of the basic GMDH polynomial, Eq. (1), in approximately 1 ms on average. The calculation of both, the flowrate and the properties of the natural gas with fixed composition, takes up to 870 ms in our FC prototype. In order to ensure the completion of the flowrate calculation and the corresponding correction safely within the 1000 ms measurement cycle we limited the ET of the flowrate correction to 50 ms. When generating the GMDH model, the RRSE threshold of the flowrate correction factor will be decreased as long as it provides the generation of at least one model satisfying the ET threshold. By setting the ET threshold to 50 ms, the maximum number of layers to 15 and by varying other parameters of the GMDH algorithm we were able to create the satisfactory models of the flowrate correction factor with the RRSE below 4.0 %.
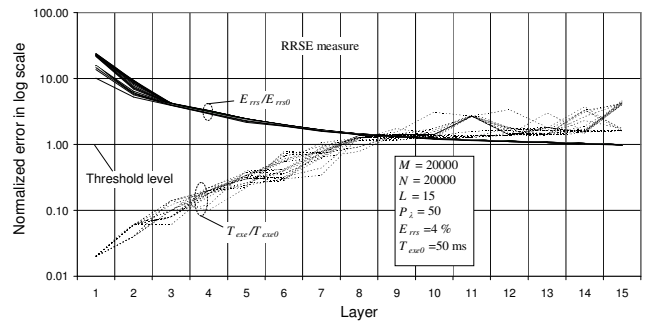
Fig. 6. Illustration of the GMDH algorithm with RRSE measure, Eq. (11), failing to find the satisfactory model for the flowrate correction factor K_q. The RRSE (solid lines) and ET (dotted lines) for the best 20 models at each layer are normalized to their respective thresholds. The algorithm uses the training and the validation data set each consisting of 20000 samples. The maximum number of qualified polynomials per layer is set to P_λ=50 for each layer, λ=1,...,15, the average ET of the basic GMDH polynomial is set to 1 ms, and the thresholds, Eq. (10), are set to E_{rrs0}=4.0% and T_{exe0}=50ms. The ET lines of all models exceeded the threshold before any of the RRSE line dropped below it and the algorithm failed to find an acceptable model.

Fig. 5 illustrates how the CE measure, Eq. (12), forces the algorithm to decrease the RRSE of the model by controlling the increase of its ET. Fig. 5 shows that the RRSE of at least one model (solid lines) drops below the threshold (normalized error = 1) before any of the ET (dotted lines) exceeds it and the algorithm finds the satisfactory model at layer 15. We varied the weighting coefficient c_w in Eq. (12) in the range
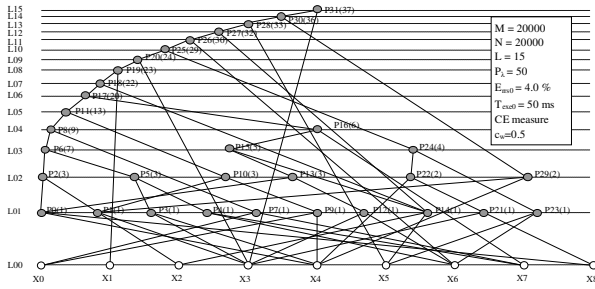
Fig. 7. Polynomial graph of the best GMDH surrogate model of the flowrate correction factor K, obtained at layer 15 by using the CE measure Eq. (12) with weighting coefficient c_w=0.5 and with the threshold levels, Eq. (10), set to E_{rrs0}=4.0% and T_{exe0}=50ms. The maximum number of qualified polynomials is set to P_λ=50 for each layer λ=1,...,15. The training and the validation data sets consist of 20000 random samples each. The obtained GMDH model satisfies the given thresholds (E_{rrs}=3.967 % and T_{exe}=37 ms) and is suitable for implementation in FC software.

Table 8

GMDH polynomial model of the correction factor in recursive form with the corresponding coefficients of the second order two-dimensional polynomials

GMDH polynomial model in recursive form
$y=P_{31}(P_{30}(P_{28}(P_{27}(P_{26}(P_{25}(P_{20}(P_{19}(P_{18}(P_{17}(P_{11}(P_8(P_6(P_2(P_0(x_4,x_8),P_1(x_2,x_3)),P_5(P_3(x_3,x_4),P_4(x_6,x_7))),P_7(x_0,x_7)),P_{10}(P_9(x_0,x_4),P_1(x_2,x_3))),P_{16}(P_{15}(P_{13}(P_0(x_4,x_8),P_{12}(x_3,x_6)),P_{14}(x_2,x_5)),x_7)),P_{14}(x_2,x_5)),x_1),x_3),P_{24}(P_{22}(P_{21}(x_3,x_8),x_4),P_{23}(x_5,x_6))),x_6),P_{14}(x_2,x_5)),x_5),P_{29}(P_1(x_2,x_3),x_4)),x_3)$

Basic regression polynomial
$P_i(z_j,z_k)=a_0(i)+a_1(i)\ z_j+a_2(i)z_k+a_3(i)\ z_jz_j+a_4(i)\ z_kz_k+a_5(i)z_jz_k$

Coefficients of the polynomials P_0 to P_{31}

i	a_0	a_1	a_2	a_3	a_4	a_5
0	1.0001E+0	-1.1357E-2	-6.8704E-4	2.5536E-4	8.0474E-4	8.4350E-3
1	9.8856E-1	-3.3090E-4	6.7325E-5	7.0360E-6	-1.0142E-7	7.3114E-7
2	-8.1858E+2	7.4253E+2	8.9596E+2	5.0943E+1	8.5870E+1	-8.4398E+2
3	9.9012E-1	6.6260E-5	-4.1345E-2	-1.1050E-7	-2.7501E-5	1.1208E-4
4	1.0005E+0	5.2566E-3	-1.0140E-4	-5.5278E-3	9.3191E-7	4.1835E-6
5	-4.9380E+1	-3.2481E+1	1.3133E+2	-1.5787E+1	-9.7756E+1	6.5075E+1
6	-1.6081E+2	2.4385E+2	7.9023E+1	-1.7140E+1	6.5044E+1	-2.0896E+2
7	9.9774E-1	7.4210E-3	1.0690E-4	-6.6765E-3	-1.7098E-6	-2.4801E-4
8	-1.2395E+3	1.2696E+3	1.2113E+3	-3.1377E+1	-2.2670E+0	-1.2068E+3
9	9.9999E-1	8.5310E-4	-7.3055E-3	-7.3184E-3	4.8341E-4	-1.1245E-2
10	-4.3539E+2	1.2580E+3	-3.8654E+2	-1.0374E+2	7.1916E+2	-1.0505E+3
11	6.0579E+1	-8.4832E+1	-3.5432E+1	7.7879E+1	5.2456E+1	-6.9650E+1
12	9.8649E-1	6.4671E-5	5.4189E-3	-1.0113E-7	-7.4088E-3	1.0893E-5
13	-2.5121E+2	8.1232E+2	-3.0962E+2	4.1247E+1	6.0267E+2	-8.9441E+2
14	9.9954E-1	3.3668E-4	-5.4531E-5	-1.9968E-5	-2.5227E-9	3.5061E-6
15	-2.7176E+2	3.6409E+2	1.8065E+2	1.0868E+1	1.0229E+2	-3.8514E+2
16	-6.1959E+1	1.2610E-2	-2.8801E-2	-6.3142E-1	5.4548E-7	2.8761E-2
17	-3.0692E-1	1.6415E+1	-1.4806E+1	-1.8346E+1	-2.8921E+0	2.0936E+1
18	-1.8777E+2	1.1482E+2	2.6201E+2	6.4193E+1	-9.9645E+0	-2.4228E+2
19	-7.8929E+0	1.6780E+1	1.0244E+0	-7.8875E+0	5.9509E-3	-1.0252E+0
20	1.6250E+0	-2.4087E+0	5.0903E-4	1.7861E+0	2.4507E-8	-5.2458E-4
21	9.8493E-1	7.8212E-5	3.7369E-3	-1.0339E-7	8.8817E-4	-1.2276E-5
22	-8.8257E+1	1.7868E+2	-1.0451E+1	-8.9419E+1	-2.5096E-4	1.0451E+1
23	9.9690E-1	-3.3893E-6	8.3911E-3	-3.1845E-9	-6.8053E-3	-8.7023E-7
24	-8.0245E+2	6.4401E+2	9.6266E+2	2.1901E+1	-1.3782E+2	-6.8731E+2
25	2.0536E+1	1.4721E+2	-1.8732E+2	-1.2442E+2	4.2649E+1	1.0234E+2
26	-1.1994E+1	2.4927E+1	1.3707E-1	-1.1932E+1	7.7668E-4	-1.3829E-1
27	-3.3928E+1	-4.8502E+1	1.1742E+2	-2.0110E+1	-1.0364E+2	8.9758E+1
28	3.3045E+0	-5.6009E+0	-2.2026E-4	3.2964E+0	6.1967E-9	2.1961E-4
29	5.6656E+1	-1.1139E+2	-9.6569E+0	5.5730E+1	8.1188E+0	9.6565E+0
30	7.6042E+0	8.0651E+0	-2.2283E+1	1.6229E+0	1.6282E+1	-1.0291E+1
31	1.0721E+1	-2.0678E+1	7.3476E-4	1.0958E+1	8.2460E-9	-7.4024E-4

from 0 to 1 in 0.1 steps and the best models have been obtained for equally balanced error terms, i.e. for c_w=0.5.

Fig. 6 demonstrates how the RRSE measure, Eq. (11), fails to find a satisfactory model by forcing the algorithm to minimize the RRSE only, while leaving the increase of the ET uncontrolled. The identical results can be obtained when using the CE measure, Eq. (12), with c_w=1. Figs. 5 and 6 illustrate the general patterns of model search using CE measure, Eq. (12), and RRSE measure, Eq. (11), respectively.

Fig. 7 illustrates a polynomial graph of the best GMDH surrogate model of the flowrate correction factor obtained at layer 15 when using the CE measure, Eq. (12). The RRSE (E_{rrs}=3.967%) and the ET (T_{exe}=37 ms) of the model are both below the given thresholds (E_{rrs0}=4.0% and T_{exe0}=50 ms) making the model suitable for implementation in our FC prototype. The CE measure proves to be very efficient in tailoring the model for real time systems since it optimizes the model with respect to the approximation error and the complexity.

The recursive equation of the flowrate correction factor model (Fig. 7) with the corresponding coefficients of the basic polynomials, truncated to 5 most significant decimal digits, are shown in Table 8, where $x_0,...,x_8$ denote the input parameters shown in Table 7.

When using the RRSE instead of CE measure under the same conditions, the RRSE error (E_{rrs}=3.915 %) of the best model obtained at layer 15 falls below the threshold but the corresponding ET (T_{exe}=197 ms) exceeds the given threshold significantly making the model too complex and therefore unsuitable for implementation in the FC prototype.

7. Results and discussion

In this section, the applicability of the obtained GMDH model for the compensation of JT effect in real-time flowrate measurements is verified. The accuracy and the precision of the derived model was tested on 10 randomly generated validation data sets, each consisting of 20000 samples, and the summary of the results is shown in Table 9. Thus, from Table 9 it can be seen that the standard deviation equals approximately 1% of the corresponding average value of RMSE and RRSE and we may conclude that the derived correction factor approximates the correction procedure consistently in the entire range of application.

Fig. 8 illustrates the results of the simulation of a relative error $E = (q_d - q_u)/q_u$ in the measurement of the natural gas flowrate when ignoring the effect of the temperature drop due to the JT expansion (q_d), instead of its precise correction (q_u) in accordance with the procedure outlined in Table 1. The calculation of the flowrate is simulated by assuming the square-edged orifice plate with corner taps [3], with orifice diameter of 20 mm, the pipe diameter of 200 mm, the differential pressure of 0.2 MPa, and with the downstream measurement of the temperature. The error corresponds to the natural gas with the following mole fractions: *nitrogen*=0.009617, *carbon dioxide*=0.015021, *methane*=0.959284, *ethane*=0.084563, *propane*=0.023022, *n-*

butane=0.006985, *n-pentane*=0.001218, *n-hexane*=0.000228, *n-heptane*=0.000057 and *n-octane*=0.000005). The natural gas

Table 9
Errors in the calculated correction coefficient when approximating the precise procedure (Table 1) by the best GMDH polynomial model (Fig. 7 and Table 8) obtained at layer 15 by using the CE criterion Eq. (12)

Validation set index	E_{rms} x10^{-5}	E_{rrs} [%]
1	2.305	4.007
2	2.267	3.939
3	2.258	3.933
4	2.225	3.910
5	2.270	3.922
6	2.303	3.999
7	2.295	3.969
8	2.273	3.968
9	2.277	3.922
10	2.280	3.966
Mean value: $\bar{x} = \dfrac{1}{N}\sum_{1}^{N} x_i$	2.275	3.954
Standard deviation: $\sigma = \sqrt{\dfrac{N\sum_{1}^{N} x_i{}^2 - \left(\sum_{1}^{N} x_i\right)^2}{N(N-1)}}$	0.02356	0.03341

is taken from Table G.1 in [6] and corresponds to the gas mixture denoted by the 'Gas 3', which produces the largest temperature changes of all six mixtures given in [6] for validation purposes. The pressure varies from 1 MPa to 12 MPa in 0.5 MPa steps and the temperature from 263 K to 333 K in 10 K steps. From Fig. 8 it can be seen that the relative error approaches 0.6 % for the temperatures close to 263 K and for the pressures close to 8.5 MPa. The relative flowrate errors obtained for the remaining gas mixtures given in Table G.1 [6] are considerably lower.
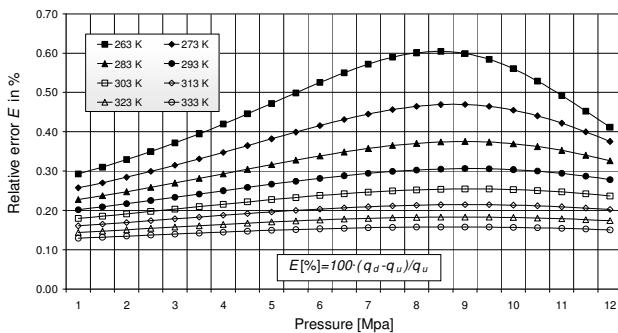

Fig. 8. Illustration of a relative error in the measurement of a natural gas flowrate by orifice plate with corner taps when ignoring the temperature drop due to the JT expansion effect.

Fig. 9 shows the correction factor, Eq. (5), for the precise compensation of the flowrate error shown in Fig. 8. The natural gas density slightly increases when decreasing the temperature and if not corrected the measured flowrate will be correspondingly higher than the actual flowrate resulting in positive flowrate error (Fig. 8). Consequently, the corresponding correction factor is close to but always less than one (Fig. 9).
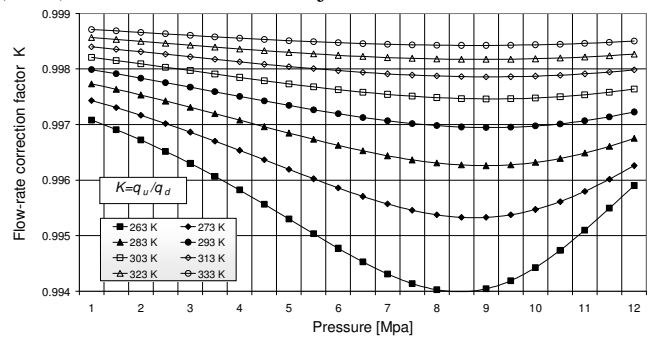

Fig. 9. Flowrate correction factor for the compensation of the flowrate error shown in Fig. 8.

Fig. 10 illustrates the relative flowrate error $E_{GMDH} = (K_{GMDH} \cdot q_d - q_u)/q_u$ when compensating the temperature drop effect by the GMDH correction polynomial, Table 8, instead of its precise correction by the correction factor shown in Fig. 9 and calculated in accordance with the procedure outlined in Table 1. The results are obtained by simulating the flowrate through the square-edged orifice plate with corner taps [3], with orifice diameter of 20 mm, the pipe diameter of 200 mm, the differential pressure of 0.2 MPa, and with the downstream measurement of the temperature. Again, the natural gas is taken from Table G.1 in [6] and corresponds to the gas mixture denoted by 'Gas 3'. The pressure varies from 1 MPa to 12 MPa in 0.5 MPa increments and the temperature from 263 K to 333 K in 10 K increments.
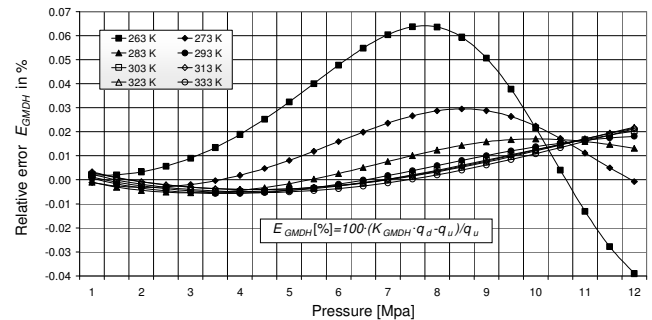

Fig. 10. Illustration of relative error in a measurement of natural gas flowrate, when using the GMDH polynomial model of the flowrate correction factor (Fig. 7 and Table 8) instead of the precise calculation procedure (Table 1).

From Fig. 10 it can be seen that the GMDH correction factor decreases the non-compensated relative error (Fig. 8) roughly by the order of magnitude in the entire pressure/temperature range. The error performance is somewhat degraded at higher pressures and at lower temperatures but the absolute value of the relative error never exceeds 0.064%. Similar results are obtained for the remaining gas mixtures from Table G.1 [6] and for various randomly generated gas compositions. Almost identical error performance characteristics are obtained when applying the same GMDH model for the correction of the JT effect in the measurements using orifice plates with corner, flange or D&D/2 taps [3] since the corresponding differences in the calculated temperature drops are negligible for the same natural gas flowing under the same operating conditions.

The non-compensated flowrate error varies by varying the natural gas composition due to the corresponding variation of

the JT coefficient. For a fixed natural gas mixture the absolute value of a JT coefficient [2][5] is increasing by decreasing the temperature, thus increasing the temperature drop, Eq. (1), which increases the uncertainty of the calculated density of a natural gas and the uncertainty of the flowrate, as well. Also, the increase of the differential pressure and the decrease of the diameter ratio are increasing the pressure loss, Eq. (2), thus amplifying the temperature change, Eq. (1), and consequently the flowrate error.

The flowrate error (Fig. 8) occurs when measuring the temperature downstream of the orifice plate and when assuming the same temperature upstream of the orifice plate [1]. The procedure for the precise compensation of a temperature drop effect (Table 1) eliminates the corresponding flowrate error completely but it needs double calculation of both the flowrate and the properties of a natural gas and is therefore computationally intensive and time consuming and may be unacceptable for low-computing power measurement systems. The above described correction procedure performs a simple scaling of the flowrate, calculated at "downstream conditions" [1], by the correction polynomial (Table 8) and is easy to calculate and to implement in software. The correction procedure slightly increases the calculation time of a common procedure [1] but it decreases the non-compensated flowrate error, due to the temperature drop, by one order of magnitude (Figs. 8 and 10). Hence, it makes the error negligible with an acceptable degradation of the calculation time.

The low-complexity GMDH polynomial is generated by optimizing the RRSE and the ET using the learning and the validation data samples uniformly distributed in the entire application space and, consequently, it approximates the correction factor more accurately in subspaces with lower non-linearity. The correction error could be further reduced by representing the non-linear regions of the correction factor by a larger number of training and validation data samples, throughout the GMDH model learning, but it is hard to construct such a data sampling in a high dimensional space.

The CE measure proves to be very efficient in tailoring the model for real time system as it optimizes the model with respect to the approximation error and the complexity. The obtained model decreases the computational complexity of the original procedure significantly while preserving reasonable approximation accuracy and is therefore applicable in low-computing-power systems.

Most likely, the obtained model (see Fig. 7 and Table 8) is not the best of all possible GMDH models because the complete search is unfeasible due to the huge number of possible models at higher layers. But, unlike RRSE measure, Eq. (11), the CE measure, Eq. (12), forces the GMDH algorithm to decrease the error while controlling the increase of ET and generally discovers more favorable solution with respect to both parameters.

8. Conclusions

The GMDH surrogate of a computationally intensive procedure for the compensation of the flowrate error caused

by the JT expansion effect is derived using the compound squared relative error measure of the accuracy and the ET (complexity) of the model. First the complete set of input parameters for the calculation of the natural gas flowrate is specified (Table 5) and the corresponding training and validation data sets are generated. The parameters are then aligned according to their impact on the approximation accuracy of the model (Fig. 3). The optimum total number of representative input parameters is established by searching for the parameters which are producing the minimum CE of the model (Fig. 4 and Table 7). Finally, the acceptable model is derived by minimizing the CE, Eq. (12), and by satisfying the predefined thresholds for the RRSE and the ET.

The derived surrogate model of the correction factor enables direct compensation of the flowrate error caused by the JT effect. Significantly reduced ET and reasonable accuracy make the surrogate model executable in real-time by low-computing-power microcomputer. The same model can be used for the compensation of temperature drop effect when measuring the flow rate of the natural gas by using orifice plates with corner-, flange- or D and D/2-taps [3], where the natural gas can be specified either by the composition [7] or by the physical properties [8].

References

[1] ISO-5167-1, *Measurement of fluid flow by means of pressure differential devices inserted in circular-cross section conduits running full,* Ref. No. ISO-51671-1:2003(E), ISO; 2003.

[2] I. Marić, "The Joule–Thomson effect in natural gas flowrate measurements," *Flow Measurement and Instrumentation*, Vol. 16, Issue 6 , December 2005, 387-395.

[3] ISO-5167-2, *Measurement of fluid flow by means of pressure differential devices inserted in circular-cross section conduits running full - Part 2: Orifice plates*, Ref. No. ISO-51671-2:2003(E), ISO; 2003.

[4] E. W. Lemmon and K. Starling, "Speed of Sound and Related Thermodynamic properties Calculated from the AGA Report No. 8 Detail Characterization Method Using a Helmholtz Energy Formulation," *American Gas Association Conference and Biennial Exhibition*, Orlando FL, April 28, 2003.

[5] I. Marić, "A procedure for the calculation of the natural gas molar heat capacity, the isentropic exponent, and the Joule-Thomson coefficient," *Flow Measurement and Instrumentation*, Vol. 18/1, March 2007, 18-26.

[6] ISO-20765-1, *Natural gas – Calculation of thermodynamic properties - Part1: Gas phase properties for transmission and distribution applications*, Ref. No. ISO-20765-1:2005, ISO; 2005.

[7] ISO-12213-2, *Natural gas – Calculation of compression factor – Part 2: Calculation using molar-composition analysis*, Ref. No. ISO-12213-2:1997(E), ISO; 1997.

[8] ISO-12213-3, *Natural gas – Calculation of compression factor – Part 3: Calculation using physical properties*, Ref. No. ISO-12213-3:1997(E), ISO; 1997.

[9] K. E. Starling and J. L. Savidge, "Compressibility Factors for Natural

Gas and Other Hydrocarbon Gases, American Gas Association (AGA) Transmission Measurement Committee Report No. 8, American Petroleum Institute (API) MPMS, chapter 14.2, second edition, November 1992.

[10] Urner, G. "Pressure loss of orifice plates according to ISO-5167," *Flow measurement and instrumentation,* 8, March 1997, pp. 39-41

[11] Reid, R. C.J. K. M. Prausnitz, and B. R. Poling: *The Properties of Gases and Liquids*, 4th ed., McGraw-Hill, New York, 1987.

[12] A. G. Ivakhnenko, "Heuristic Self-Organization in Problems of Engineering Cybernetics," *Automatica*, Vol. 6. 1970, 207-219

[13] A. G. Ivakhnenko, "Polynomial Theory of Complex Systems," IEEE Transactions on *Systems Man, and Cybernetics*, Vol. SMC-1, No.4, Oct 1971, 364-378

[14] H. R. Madala and A. G. Ivakhnenko, *Inductive Learning Algorithms for Complex Systems Modeling*, CRC Press Inc., Boca Raton, AnnArbor, London, Tokyo, 1994.

[15] S. C. Chapra and R. P. Canale, *Numerical Methods for Engineers*, 3rd ed., McGraw-Hill, New York, 1998.

[16] I. Marić and I. Ivek, "Building GMDH Models for Real-Time Applications," (Unpublished results), http://isano.irb.hr/temp/gmdh_ce.pdf.

[17] Schouten, J. A., Michelis, J. P. J., Jaeschke, M. " Calculation of acompressibility Factor of Natural Gases Based on the Calorific Value and the Specific Gravity", Int. J. Thermophys., 11 (1), pp. 145-156

[18] Jaeschke, M., Audibert, S., Van Caneghem, P., Humphreys, A.E., Janssen-Van Rosmalen, R.,Pellei, Q., Schouten, J.A., Michelis, "Simplified GERG Virial Equation for Field Use", SPE Product Eng., 6 (3), 1991, pp. 350-355.

[19] ISO 6976, *Natural gas - Calculation of calorific values, density, relative density and Wobbe index from composition*, Ref. No. ISO-6976:1995(E), ISO; 1995.